LITHIUM DEPLETION IN PRE-MAINSEQUENCE SOLAR-LIKE STARS

L. PIAU and S. TURCK-CHIEZE

piau@cea.fr, cturck@cea.fr

CEA/DSM/DAPNIA/Service d'Astrophysique, CE Saclay, 91191 Gif-sur-Yvette Cedex 01, France

ABSTRACT

We examine the internal structure of solar-like stars in detail between 0.8 and 1.4 $M_{\odot}$ and during pre-main sequence phase. Recent opacity computations of OPAL along with a new hydrodynamical mixing process have been considered. We also introduce up-to-date nuclear reaction rates and explore the impact of accretion, mixing-length parameter, non-solar distributions among metals and realistic rotation history. We compare models predictions of lithium depletion to the ^7Li content observations of the Sun and to 4 young clusters of different metallicities and ages. We show that we can distinguish two phases in lithium depletion: 1- a rapid nuclear destruction in the T-Tauri phase before 20 Myrs : this is independent of the mass used within our range but largely dependent on the extension and temperature of the convective zone, 2- a second phase where the destruction is slow and moderate and which is largely dependent on the (magneto)hydrodynamic instability located at the base of the convective zone.

In terms of composition, we show the interest on considering helium and especially the mixture of heavy elements : carbon, oxygen, silicium and iron. We outline the importance of O/Fe ratio. We note a reasonable agreement on lithium depletion for the two best known cases, the Sun and the Hyades cluster for solar-like stars. Other clusters suggest that processes which may partly inhibit the predicted premainsequence depletion cannot be excluded, in particular for stars below $\sim 0.9 M_{\odot}$. Finally we suggest different research areas such as initial stellar models and more realistic atmospheres which could contribute to a better understanding of this early phase of evolution and which should become the object of subsequent research.

Subject headings: Stars: pre-main sequence, abundances, interiors, rotation—Convection

1. INTRODUCTION

Dynamical effects have been mainly ignored in classical stellar evolution during several decades even if they have been explored theoretically (Zahn 1974, 1992). Nowadays, helioseismology provides observational constrains on such effects and therefore allow us to begin to introduce them in the description of main sequence stars (Frolich et al. 1997; Gabriel et al. 1997; Kosovichev et al. 1997). It permits observations of the solar convective layers complex motions. Moreover acoustic mode determination allows the extraction of the rotation and sound speed profiles down to the energy-generation core (Kosovichev et al. 1997; Dziembowski 1998; Turck-Chièze et al. 1997). Meridional circulation begins to be accessible to the solar seismic observations and some (magneto) hydrodynamical instability has been put in evidence at the base of the convective zone. In order to see the consequences of such a process, we have focused our attention on two elements ^7Li and ^9Be which are destroyed in stars from the center to regions located slightly below the natural transition between transport of energy by radiation and by convection. Lithium surface abundances history is directly related to physical processes in this region which is at the same time important for understanding dynamos in stars and also probably the role of the internal magnetic field in

general. Brun, Turck-Chièze, & Zahn (1999) have invoked the hydrodynamical instability proposed by Spielgel & Zahn (1992) to explain both recent helioseismic results and the solar lithium depletion. They introduced a turbulent term in the equation of diffusion. This term is directly related to local rotation and differential rotation. Evolution of such a mixing term with recorded surface rotation history of sun-like stars in open-clusters finally explains the present observed solar photospheric element abundances. It also produces the right order of magnitude of lithium destruction as a function of time for open-clusters older than a Gyr (NGC 752, M67).

In this paper we focus on the different ingredients of the mainsequence (MS) and above all premainsequence (pre-MS) structural evolution of solar-like stars through the excellent indicator which is the ^7Li surface abundance. From that viewpoint stellar evolution models have received a lot of attention for a long time. Almost forty years ago pre-MS evolution was already proposed to explain the low solar ^7Li abundances relative to the solar system value as well as field stars and Hyades depletion pattern with temperature (Bodenheimer 1965). Bodenheimer described the main features of lithium burning in pre-MS. Accurate ^7Li observational data for open clusters have similarly been obtained for long (Zappala 1972). They have outlined the complex history of this element and suggested depletion with age on MS. In the past twenty years many theoretical and observational works have addressed the topic. These investigations suggested that the understanding of lithium abundance might be related to many different non-standard processes extending from microscopic diffusion (Michaud 1986) to large scale mixing through rotation (Baglin et al. 1985) angular momentum evolution (Pinsonneault et al. 1989) or internal waves (Schatzmann 1993). During pre-MS lithium depletion strongly depends on typical temperatures within convection zones and therefore input physics (Profitt & Michaud 1989). Until today there is no safe explanation of lithium history among solar-like stars. It is very likely that various phenomena are indeed responsible for pre-MS and MS ^7Li evolution as well as G-type stars depletion pattern and lithium dip. This controversial subject therefore remains a broad and active area of research (D'Antona & Mazzitelli 1994, 1997; Ventura et al., 1998; Palla 1999; D'Antona, Ventura & Mazzitelli, 2000).

This work intends to show results involving recent opacity and nuclear reaction rates determination. We consider possible variations of composition and non solar repartition among metals as in the next decade many improvements in the knowledge of the detailed photospheric composition of the young stars are anticipated. We envision variations of mixing-length parameter with age and a new hydrodynamical instability along with a realistic rotation evolution. We outline the impact of such improvements on the topic of early phases of evolution which is meant to be better constrained by future seismic informations. In section 2, we describe the bases of the stellar models we use and examine the solar case in details. The role of the different elements through their composition and the opacity coefficients is discussed in details in section 3. Section 4 is dedicated to convection & accretion and section 5 to rotation. Finally we give some perspectives in section 6.

2. PRE-MAIN SEQUENCE EVOLUTION OF SOLAR-LIKE STARS

2.1. Physics and global evolution

In this study, we consider models in the mass range from 0.8 to 1.4 $M_\odot$ and different compositions corresponding to the Sun, the Pleiades, and the Hyades. Our starting point is a fully adiabatic polytrope with a central temperature of $\sim$ 3 10^5 K and a radius of 20 $R_\odot$ for $1M_\odot$ star. So the computation begins prior to deuterium burning which corresponds to the observed birth-line (Stahler 1988). We observe that models are still fully convective polytropes when the star reaches the birth-line with a radius of about 6 $R_\odot$ so we expect no consequences of this early-phase computation except the idea to take as an hypothesis an initial polytropic structure.

Models have been computed using the CESAM code (Morel 1997) and all the updated physics useful for the refined solar models (see Brun, Turck-Chièze, & Morel 1997). For the reaction rates of the pp chain and CNO cycle, we consider the compilation of Adelberger et al. (1998) and for the $^7Li(p,\alpha)^4He$ the work of Engstler et al. (1992). We use OPAL equation of state (Rogers, Swenson, & Iglesias 1996) and opacities (Iglesias &

Rogers 1996) above 5800K. For lower temperatures the OPAL equation of state is replaced by the MHD equation of state (Mihalas, Dappen, & Hummer 1988) and the opacities are from Alexander & Ferguson (1994). Interpolation of opacities are performed using v9 birational spline package of Houdek (Houdek & Rogl 1996). The atmosphere is connected to the envelope at optical depth 10 where the diffusion approximation for radiative transfer becomes valid (Morel et al. 1994). The opacity atmospheric is Rosseland mean opacity extracted from Alexander & Ferguson (1994) or Kurucz (1992) sets. We therefore do not use grey approximation. Surface boundary conditions are $\rho = 3.55\,10^{-9} g.cm^{-3}$ when $\tau = 10^{-4}$. Standard mixing-length theory is applied and the convection zone is completely chemically homogeneous.

During the pre-MS, stars are in quasi-hydrostatic equilibrium and slowly contract towards ZAMS within a time scale comparable to their Kelvin-Helmoltz time-scale. Defining ZAMS as the age where the thermonuclear hydrogen fusion provides 99% of stellar energy the pre-MS lifetime varies from 30 Myrs for a star of 1.4 $M_\odot$ Pleiades composition up to 100 Myrs for a 0.8 $M_\odot$ star of the Hyades composition. The Sun lies in between, with a pre-MS of $\sim$ 50 Myrs. The transition from fully convective object to radiative core structure depends on mass and composition. Higher mass stars contract faster, increase internal temperatures faster and so decrease radiative thermal gradients faster. Moreover lower metallicity accelerates contraction and decreases opacities which also favor radiative stratification. Therefore lower metallicities and higher masses give rapid raise to radiative core. A massive (1.4 $M_\odot$) Pleiades composition star develops radiative core after 0.85 Myrs and a 0.8 $M_\odot$ Hyades composition star after 3.5 Myrs. In the solar case, radiative core exceeds 1% of total mass at 1.8 Myrs and then fastly accelerates in mass and radius to reach dimensions very close to its actual dimensions at 25 Myrs.

Due to the swift convective movements, surface matter is repeatedly exposed to physical conditions that prevail in deep interior. Figure 1 illustrates this point in showing the time dependent evolution of the thermodynamical quantities (temperature and density) at the base of the convection zone (hereafter BCZ) in regard to the photospheric lithium for the case of a young Sun. At the be-

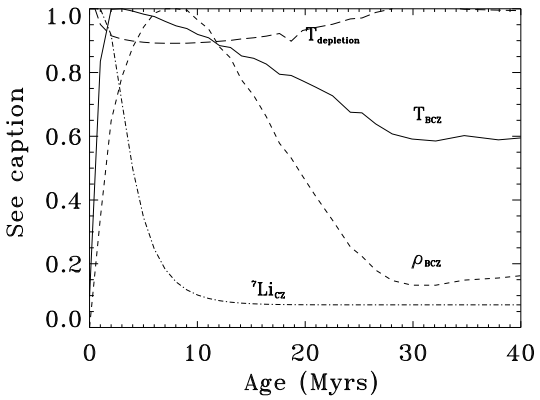

Fig. 1.— Time evolution of the temperature (continuous line) and density (dashed line) at BCZ for a 1 $M\odot$ star of solar composition. Both temperature and density are normalized to their maximum values, respectively 3.94×10^6 K and 1.97g/cm^3. We have also mentioned the density dependence of the temperature for a characteristic burning time of 1 Myrs (long-dashed line) and the lithium photospheric fraction (dot-dashed line) normalised to maximal value 9.3×10^{-9} in mass fraction (ie 3.2 dex).

ginning of the considered evolution BCZ (which coincides with the stellar center) is too cool to allow lithium burning. As the star evolves on pre-MS, deep regions of convection zone temporally exceeds ^7Li burning point in typical stellar conditions ($\sim 2.5\,10^6 K$). ^7Li therefore offers a direct insight over stellar internal structure and evolution as it is extremely sensitive to the appearance of the radiative core. We note that early ^7Li depletion occurs in the very beginning of pre-MS. Effectively, for $1 M_\odot$, the BCZ temperature increases rapidly from less than 10^6 K to approximately 4 10^6 K at 2 Myrs, the density increases also (but not quite simultaneously) up to 2 g/cm^3 between 7 and 8 Myrs. Then they slowly sink towards values which are very near from the conditions of the BCZ of the present Sun. This evolution results in ^7Li burning from 2 to 20 Myrs. The way depletion occurs presents several difficulties. First, depletion takes place just at the BCZ as convection rapidly recedes in mass-fraction passing from the whole star mass at 1 Myr to less than 20% 20 Myrs later. Moreover depletion typical time evolves rapidly and decays to very low values compared to time scale evolution of the stellar structure down to $\sim 10^5$ years at BCZ. These pecularities impose small time step and very thin meshes. Computations suggest that one third difficulty must arise. Early radiation zone stratification hardly differs from convection stratification. In other words the newly stabilized medium is (and stays for at least 10 Myrs) close to convective instability. We can illustrate this using polytropes : the adiabatic polytrope ($P \alpha \rho^{1+1/n}$ with n=3/2) is 'harder' than its radiative counterpart ($P \alpha \rho^{1+1/n}$ with n=3). Radiation zone which represents half of the stellar mass at 10 Myrs, should there be more concentrated in the core. Figure 2 shows the contrary. The fact that radiation energy transport replaces convective motions does not mean that radiative stratification immediately establishes. At 10 or 20 Myrs the stratification in radiation zone is still very close to adiabatic stratification. This has consequences on rotation evolution as we shall see in section 5. We believe this property to be related to Kelvin-Helmoltz time value. The stellar interior needs at least this long to redistribute thermal energy and evolve from convective to radiative structure. This suggests that little modifications in stellar structure or new phenomena taken into account could easily change BCZ position at times from 10 to 20 Myrs. We may for instance suppose that even a low energy density magnetic field would stabilize or destabilize the region. This point leaves a priori room for many non-standard mechanisms that will have to be investigated and that will probably lead to substantial variations in pre-MS surface ^7Li depletion (Ventura et al. 1998).

2.2. Adjustment of evolution parameters for ^7Li burning

^7Li reaction rate is extremely sensitive to temperature. For typical pre-main sequence conditions, at the maximum temperature of BCZ (3.5 to 4 10^6 K) this rate varies as T^{18} to T^{19}. The depletion is therefore very sensitive to conditions near the base of the convection zone (figure 3). Consequently, the photospheric ^7Li depletion strongly depends not only on the mass of the convection zone but also on the precision of the mass shell division at BCZ. This point is essential to perform valid integrations. We have adjusted the mesh in order to limit the variation of the reaction rate at BCZ between two layers to 15 %, this corresponds typically to meshes of 0.005 $M_\odot$ or 0.003 $R_\odot$. Moreover, the typical ^7Li pre-MS burning requires also a very accurate resolution relative to time integration. Figure 3 shows the evolution of the characteristic time along the evolution. At 3-4 Myrs we find a characteristic destruction time at BCZ of only 8.10^4 to $1.3\,10^5$ years (depending on composition). So we have adjusted the typical time step to be a factor 10 lower than the characteristic depletion time. In figure 3 we have shown three conditions corresponding to the maximum of the temperature at BCZ (3 Myrs), to the arrival on ZAMS and to the present age of the Sun. For each condition, the depletion time varies by approximately one order of magnitude from BCZ to the right end of the plot but this extension corresponds to only 10 % variation of the mass of the convection zone.

2.3. Solar lithium burning during pre-mainsequence

Pre-MS ^7Li depletion within stars of roughly solar mass and composition has been estimated in various previous investigations (Bodenheimer 1965; D'Antona & Mazzitelli 1984 ; Profitt &

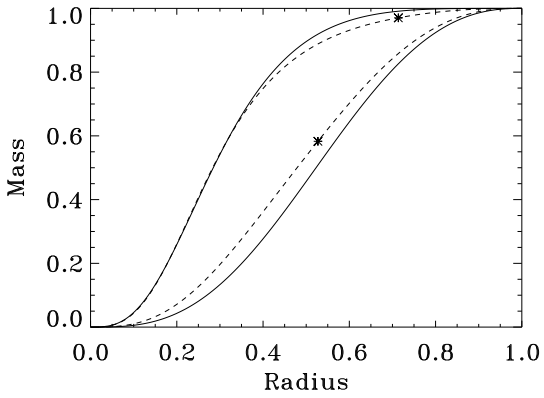

Fig. 2.— Solid lines present the mass distribution of polytrope vs radius for a $1M_{\odot}$ star. Upper solid line corresponds to a polytrope of index n=3 (representative of radiative stratification), lower solid line corresponds to a polytrope of index n=3/2 (adiabatic stratification). Dashed-lines present model stratifications at 10 Myrs (lower line) and 30 Myrs (upper line) for solar composition and mass. Crosses on these lines are BCZ. It is note worthy that at 10 Myrs stratification is still almost adiabatic albeit more than 50% of stellar mass is in the radiation zone.

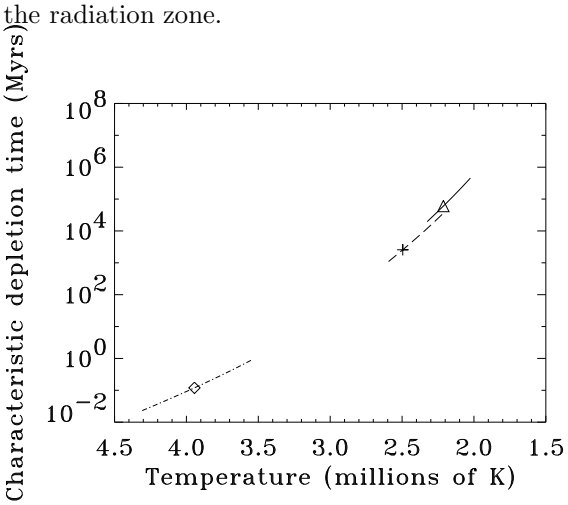

Fig. 3.— Temperature dependence of the ^7Li depletion characteristic time around BCZ for a diffusive solar model (X=0.70821, Y=0.2722). The continuous line corresponds to the solar age, dashed line to the ZAMS position, and dot-dashed line to a 3 Myrs star. Triangle, cross, and diamond represent the positions of the BCZs.

Table 1: Ratio of lithium fraction to initial fraction after pre-MS depletion phase within solar composition stars (see text for details). Our results (PTC01) are compared to previous ones of D'antona & Mazzitelli 1984 (D'A&M84), Profitt & Michaud 1989 (P&M89) and Ventura et al. 1998 (V98). P&M89a and P&M89b respectively corresponds to Z=0.0169 and 0.024. For 1.1&1$M_{\odot}$ no depletion is predicted on MS. For $0.9M_{\odot}$ star D'antona & Mazzitelli do not predict depletion on MS but Profitt & Michaud 1989 and us predict it. For these low mass stars lithium fraction therefore refers to a fixed age of 70 Myrs. Results of Ventura et al. 1998 are provided here only for solar mass stars as they do not give results for other masses in MLT framework.

Mass ($M_{\odot}$)	0.9	1	1.1
D'A&M84	0.664	0.871	0.949
P&M89a	0.467	0.679	0.823
P&M89b	0.118	0.317	0.535
V98		0.026	
PTC01	0.002	0.071	0.244

Michaud 1989; Ventura et al. 1998). These three last studies suggest lithium depletion to increase as input physics is updated. D'Antona & Mazzitelli 1984 find that a solar mass star depletes $\sim$ 13% of its initial lithium. The authors choose Y=0.23, Z=0.02 and $\alpha_{mlt} = 2$. Profitt & Michaud 1989 find that a solar mass star depletes from $\sim$ 32% to $\sim$ 69% of its initial lithium. These values correspond to the same $\alpha_{mlt} = 1.5$ but make different assumptions on the composition. The first one refers to Y=0.28, Z=0.0169 as the second one refers to Y=0.28, Z=0.024. Profitt & Michaud suggest that difference to D'Antona & Mazzitelli depletion rates is probably due to opacities improvements. They moreover remark that hte gap would get even wider if they were to use D'Antona & Mazzitelli parameters (Y and α_{mlt}). The gap between 1984 and 1989 results increases towards low masses and gets even wider if one considers very recent work from Ventura et al. (1998). A model from these authors having solar mass and composition (Y=0.28 and Z=0.02) and using MLT $\alpha_{mlt} = 1.55$ brings initial lithium

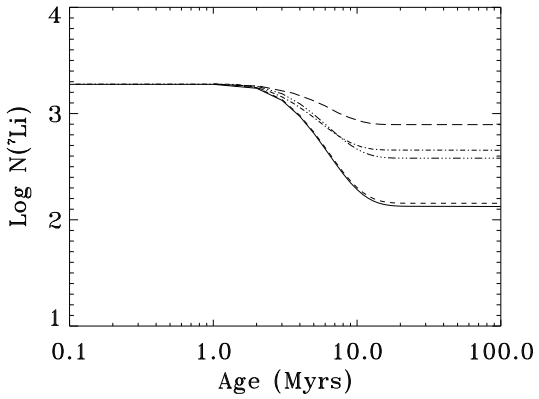

Fig. 4.— Time dependence of the photospheric ^7Li abundance for a $1M_\odot$ star with solar initial composition for different computations: a diffusive calibrated model (Y=0.2722 and Z=0.01959) with a time step adjusted to ^7Li BCZ burning time (continuous line), idem but the time step imposed by the structure of the star (dot-dashed line), a nondiffusive noncalibrated model with a time step adjusted to ^7Li BCZ burning time (dashed-line), idem but the time step imposed by the structure of the star (long-dashed line). The calibrated nondiffusive model with Y=0.2648 and Z=0.01763 with correct time step is represented by (-...-...) line and shows the effect of the composition

fraction 3.3 dex down to 1.72 dex (a decrease of a factor ~ 40). Altough a bit larger, such depletion is the same order of magnitude as what our computations suggest. The present work therefore confirms the tendency of depletion to increase with updated physics. We find that lithium lessens by roughly a factor ten in solar mass and composition star (we take Y=0.2722, Z=0.01959, α_{mlt}=1.766). Opacities must partly be responsible for this evolution but new estimations of nuclear reaction rates should also be responsible for this increase. The Engstler et al. (1992) $^7Li(p,\alpha)^4He$ astrophysical factor is indeed increased by 30 % in comparison with older values (see BTZ99). Finally the correct attention to the adapted timestep to lithium depletion rate is a third possible source of dispersion (as shown below). Table 1 compares our computations to previous ones.

Figure 4 presents the results for the evolution of the Sun in pre-mainsequence. Following the work of Brun, Turck-Chièze, & Zahn (1999, hereafter BTCZ99) we have computed models of the Sun, in introducing (or not introducing) microscopic diffusion. Depending on this choice, the initial composition Y= 0.2722, Z= 0.01959 (or Y= 0.2624, Z= 0.01763) is adjusted to get the correct luminosity and radius at the present age, calibrated with an accuracy better than $4\,10^{-4}$. Figure 4 shows that the microscopic diffusion has no effect on the pre-mainsequence. It is too slow a process as it results in a change of photospheric helium and metals abundances of only 10% along the whole life of the Sun (Turcotte et al. 1998). We have to note here a crucial point in ^7Li pre-MS depletion. Sun-like stars change much faster on pre-MS than on MS because evolutionary time scale is primarily related to contraction (hence to Kelvin-Helmoltz time τ_{KH}) which is much smaller than nuclear reaction time (τ_N). Yet one should not expect any calculation on lithium during early pre-MS to provide correct results without some cautions. Despite $\tau_{KH} << \tau_N$ forces to adopt in the code small temporal steps these are much larger than ^7Li burning time at BCZ ($\tau_{^7Li}$) at these ages. The following comparisons illustrates this. In diffusive models ^7Li depletion is increased by a factor of 3.5 between a star where time evolution is always less than one tenth of $\tau_{^7Li}$ and a model where the time step is given by the evolution of the structure. For nondiffusive models this ratio goes up to 5.3. Once time step is well below $\tau_{^7Li}$ no change in ^7Li depletion is seen at a given composition for various timesteps and with or without diffusion. In every following computations we take time step to be $\frac{\tau_{^7Li}}{10}$ as long as lithium is rapidily depleted (prior to $\sim$ 30 Myrs). Furthermore burning rate is mass-averaged over convection zone. We have checked that the results are robust to the choice of time step. If we decrease time step down to $\frac{\tau_{^7Li}}{30}$: ^7Li depletion increases of only 3.5 %. With time step adjusted for a good treatment of ^7Li burning, the difference of about 0.5 dex after 20 Myrs (a factor 3 in destruction) between diffusive and nondiffusive models is only due to the change of initial composition. This shows the great dependence of the lithium burning on the composition (see next section). Such precise computation of the lithium burning in the pre-mainsequence was not included in the previous work of BTCZ99.

Of course the notion of calibration between diffusive and nondiffusive models is not justified in the study of young clusters but the great sensitivity of this calibration shows already the difficulty of predicting lithium burning in pre-mainsequence stage.

^7Li is generally not the only probe of the stellar internal structure but ^6Li is depleted at lower temperature and is of no help here. We have observed that ^9Be burning gives similarly poor indications. In fact, computed stellar models of 0.8 to 1.4 $M_\odot$ show a ^9Be depletion of less than 0.04 dex whatever the cluster membership (from Pleiades to Hyades).

3. THE ROLE OF THE DETAILED COMPOSITION

3.1. Open cluster evolution

Open clusters allow a direct test of ^7Li evolution with time and/or composition. In this paper we focus our attention on two young and two midle-age clusters : Pleiades and Blanco I (ζ Sculptoris) for the former Hyades and Coma Berenices for the latter. The objective is to distinguish metallicity from age effects. Blanco I and the Hyades apparently are metal-rich clusters with respectively $[Fe/H] = 0.127 \pm 0.022$ (Boesgaard & Friel 1990) and $[Fe/H] = 0.14 \pm 0.01$ (Jeffries & James 1999) however Blanco I is much younger than the Hyades and with an age around 50 to 90 Myrs comparable to the Pleiades cluster which is estimated to be 70 Myrs old (Patenaude et al. 1978). On the other hand Pleiades and Coma Berenices clusters have metallicities very slightly below solar one with $[Fe/H] = -0.034 \pm 0.024$ (Boesgaard & Friel 1990) and $[Fe/H] = -0.052 \pm 0.026$ (Friel & Boesgaard 1992) respectively but Coma has an age of 500 Myrs comparable in age to the old Hyades cluster of $\sim 600 Myrs$ (Perryman et al. 1998). It should be mentioned that composition data are undoubtedly more reliable in the case of Hyades or Pleiades than in the case of Blanco I which is more distant ($\sim 250 \pm 30 pc$) than all other clusters and has been less studied.

Unlike the sun, microscopic diffusion has a negligible effect in the evolution of these young or midle-age clusters. We compute a decrease of 1.3 and 0.8 % for helium and metals in Hyades solar mass star case. As such variations always remain largely smaller than error bars over metallicity or helium content it is immaterial to study initial composition effect resulting from diffusion. This is particularly true for lithium. Let us however remark that microscopic diffusion time appears roughly ten times shorter for F type stars. We compute a decrease of respectively 10% and 6% for helium and metals in $1.4 M_\odot$ ($T_{eff} \sim 6600K$) at Hyades age. However at an age of 50 Myrs decrease of helium and metals are only 0.6% and 0.4% so that it is not plausible that microscopic diffusion changes early lithium history even in case of slightly more massive stars than the sun.

In this study, we do not consider different initial ^7Li abundances. In all four clusters stars more massive than 1.4 solar masses (Teff>6900 K) exhibit the same ^7Li content of 3.2 to 3.3 dex for Pleiades, Hyades, (Soderblom et al. 1993) and Coma (Boesgaard 1987) . Blanco I depletion pattern is furthermore identical to Pleiades' one (Jeffries 1999). The early F-stars abundances remain unchanged and are compatible both with very young T Tauri stars (Magazzu, Rebolo, & Pavlenko 1992) and the interstellar medium present ^7Li value (Knauth et al. 2000). Indeed, it seems that there was no significant evolution in galactic gas ^7Li/hydrogen ratio over the last 1.7 Gyr (Hobbs et al. 1988) so that the initial ^7Li does not vary from Hyades formation time until today. For all the clusters we take the same standard value of 3.27 dex for initial ^7Li abundances.

In the following we will investigate the effects of the composition on the lithium burning in separating the effects of deuterium, helium, and metals.

3.2. Sensitivity of the lithium burning to the deuterium composition

Deuterium, the most fragile element, is depleted around $5\,10^5$ K in stellar interiors. The galactical evolution leads to a continuously decrease because of astration. Recent measurements show an abundance of $(D/H)_{ISM} = 1.46 \pm 0.09 \times 10^{-5}$ (Piskunov et al. 1997) or $(D/H)_{ISM} = 1.60 \pm 0.09 \times 10^{-5}$ in direction of Capella (Linsky et al. 1995) whereas presolar value is estimated as $(D/H)_{pre\odot} = 3.01 \pm 0.17 \times 10^{-5}$ by Gautier & Morel (1997). Young clusters initial abundances are probably the same as present ISM one.

During contraction, the stars experience several stages of light element burning. First, deuterium burning ($T = 5\,10^5$ K) significantly participates to the energy production. Palla & Stahler (1991) have shown that for 1 $M_\odot$ star, deuterium burning stops the contraction at a radius of $\sim 5 - 6R_\odot$ which defines the so called birth-line (Stahler 1988). The deuterium burning stops before 1 Myr when first phase lithium depletion starts. Consequently the star should have enough time to 'forget' its previous history. We checked this briefly in the framework of our models. For solar mass stars, deuterium begins to burn at the age $\sim 4\,10^4$ years during $\sim 2\,10^5$ years duration. Then lithium depletion starts after $1.4\,10^6$ years shortly prior to radiative core appearence. We have considered three deuterium mass fraction: the solar value, the actual ISM value and also a null value. Such variations hardly change lithium photospheric abundances evolution. Models having Hyades or Pleiades composition, show maximum variations between them of $\sim 10\%$ (0.04 dex) up to clusters or solar ages. When deuterium fraction decreases, lithium depletion slightly increases.

3.3. Sensitivity of lithium burning to the helium content

^7Li evolution is sensitive to metals but also to helium mass fraction. The solar photospheric helium has been determined by helioseismology to be 0.246-0.249 (Basu & Antia 95). Including microscopic diffusion (partly inhibited by turbulence) in calibrated solar models provides a mean to reach the initial solar helium content, estimated to be 0.2722 (BTCZ99). For open clusters there is no recent helium abundance determinations for any studied cluster except the Hyades. A ZAMS low mass stars fit of Hyades suggests the cluster helium fraction to be 0.26 ± 0.02 (Perryman et al. 98). This value is confirmed by the position of a number of Hyades binaries in M-L diagram (Lebreton 2000). We adopt this value in our calculations. However other calculations (Pinsonneault et al. 1998) suggest an higher value of 0.283. For the other clusters we use the usual helium to metallicity scaling law : $\Delta Y/\Delta Z = 3 \pm 2$ as deduced from calibration of nearby visual binary systems (Fernandes et al. 1998). In the same manner evaluations based on HII regions suggest an increase of helium content with metals. If we refer to figure 12 from Meyer 1989 we find that $\Delta Y/\Delta Z$ lies between 1.5 and 6. Such a trend is not totally satisfactory as the Hyades do not seem to follow this law. In fact the use of such a law requires a knowledge of both helium and metallicity in at least one site which is generally taken to be our solar system neighborhood. But the solar system seems not to be representative of 4.6 Gyrs ago mean trends of the ISM (Gies & Lambert 1992) so it is possible that deduced helium fractions are biased. Other calibrations of the metal/helium relation coming from globular clusters and galactic bulge measurements do not lead to similar helium fractions (Deliyannis, Demarque & Kawaler 1990). Changes here are not so important, so we retain here solar system abundances as reference point.

We have estimated the impact of helium variation on lithium depletion around solar composition, for Pleiades age, together with reasonable variations of the mixing-length parameter α, and metal fraction. The effect of the mixing length parameter is small, an increase of 5% leads to a decrease of ^7Li content by 20%. On the contrary the impact of the composition is high: an increase of Δ Y= 0.025, leads to a decrease of lithium burning by 64%, the corresponding Δ Z = 0.025/3 leads to an increase of lithium burning by a factor 300 and the correlated variation of helium and metallicity leads to an increase of lithium burning by a factor 60. We address the metallicity dependence more precisely in the next chapter. The anti-correlation between lithium depletion and helium is reported in previous calculations. D'Antona & Mazzitelli (1984) analyse helium mass fraction 0.23 and 0.28. There the rate of lithium fraction remaining from their initial fraction to this helium mass variation ($\frac{^7Li}{^7Li_0}/\Delta Y$) is roughly 3.3 and 1.3 for 0.9 and $1M_\odot$ stars respectively. Considering a helium variation (~ 0.05) from 0.2624 to 0.32 we correspondingly find rates 2.7 and 4.7 for 0.9 and $1M_\odot$ stars. This is the same order of magnitude as D'Antona & Mazzitelli one although our dependence seems a bit larger. The sensitiveness on helium fraction can easily be understood since opacities in stellar interiors reduce with helium content : less electrons are available for the same amount of matter. If we assume that helium content is a free parameter we can speculate as to what level it should be increased to agree with the observations in Pleiades case. Lithium abundances being scat-

tered for any given effective temperature one has first to derive a mean value. Figure 5 (dashed line) shows a third degree polynomial least square fit of observed abundances. We obtain helium fraction of 0.36 for $0.85 M_{\odot}$ star, 0.32 for $1 M_{\odot}$, and 0.3 for $1.4 M_{\odot}$. These very high values seem difficult to justify. Recent work by Deharveng et al.(2000) on helium abundances in HII galactic regions shows He/H to be below 0.105 where it can safely be determined from He^{+}/H^{+} ratios. This corresponds to helium mass fraction below 0.3. Another work indicates helium mean mass fraction should be 0.28 ± 0.02 in the galactic bulge (Minniti 1995) which is probably an upper limit to galactic abundances as most chemically evolved stars populations are expected to be near the center of our galaxy. A second difficulty is that helium mass fraction would have to vary with mass by about 20%. This certainly is not what we observe in Pleiades. Nevertheless, it is clear from this analysis that a proper determination of helium is a crucial knowledge to understand the young clusters lithium evolution.

3.4. Sensitivity of lithium burning to the metallicity

We have computed several models to describe the 1 $M_{\odot}$ Hyades and Pleiades stars. These models rely on physics described in section 2.1. Table 2 summarizes these results. We have calculated three types of models: the first one (A) uses metallicity deduced from the observation of iron given in section 3.1 and α parameter calibrated on solar models (1.766). The second model (B) adopts the same composition but three different values of α were used to account for recent 2D hydrodynamical evaluations (see section 4.1). The third model (C) is an extremal model in the sense that it adopts the lowest metallicity and highest helium content within error bars in an attempt to cancel discrepancies between calculations and observations. In the Hyades case we have added a supplementary model (D) introducing the value of 0.283 in helium mass fraction claimed by Pinsonneault et al. 1998. Other Hyades models have been computed, we discuss them in more detail in section 3.5

On the main sequence effective stellar temperatures evolve slowly. The temperature of an open cluster solar mass star will therefore be reliable independently on age uncertainties. Moreover these temperatures do not vary much within composition uncertainties or α parameter different evaluation along early pre-main sequence (see table 2). For instance the $1 M_{\odot}$ Hyades models exhibits a variation of less than 10 K around 5450 K between 550 and 700 Myrs (idem for the model including α parameter effects on early pre-MS variation but around 5500 K).
We note in figures 5 and 6 that ^{7}Li depletion is too strong on pre-main sequence for solar-type stars with Pleiades or Hyades composition. This agrees with recent results from Morel et al. (2000) of the B component of ι Pegasi binary system. With an estimated age of 56 Myrs for the system and [Li]=2.69 dex for the B component this 0.819 star is clearly underdepleted. This problem is pointed out in other recent studies. Ventura et al. (1998) using the full spectrum of turbulence of Canuto, Goldman, & Mazzitelli (1996) prescription for modelling the convection found also a too strong depletion for solar composition stars, and similarly a very strong dependence on metallicity and mass.

It is well known that open cluster stars exihibit an anti-correlation between effective temperature and lithium abundances. Moreover the dispersion in lithium abundances grows when temperature declines. This dispersion is too large to be due to abundance uncertainties (Soderblom et al. 1993). This is also too large to be due to color errors as the vector of temperature errors is nearly parallel to the mean lithium-T_{eff} trend in cool open cluster stars. Moreover this dispersion is already observed in ^{7}Li equivalent width as a function of color (Soderblom et al. 1993, Thorburn et al. 1993). At a given effective temperature there is undoudtedly real star to star differences.

Observations for each star give an effective temperature and a lithium abundance but these quantities are not directly measured as they are deduced from photometric measurements such as (B-V) and equivalent width of a particular spectral absorption line. Measurements are always slightly scattered and moreover there are unavoidable errors when doing conversions. For Pleiades open-cluster, Soderblom et al. (1993) find uncertainty for effective temperature of $\sim 130K$ and uncertainty for $^{7}Li \sim 0.05$ dex. For the Blanco I cluster Jeffries & James (1999) give an effective

Table 2: $1M_{\odot}$ stellar models for Sun, Pleiades, and Hyades compositions. All models include microscopic diffusion. Several α parameter values have been considered : 1.766 is value assumed at solar age it is deduced from solar calibration. α=1.748 results from slightly different calibration when tachocline mixing is taken into account. 1.935 and 1.850 are values induced from hydrodynamical simulations (Ludwig, Freytag, &Steffen 1999). For Pleiades composition we take α=1.935 before 15 Myrs and α=1.85 from 15 to 22 Myrs. For Hyades composition we take α=1.935 before 20 Myrs and α=1.85 from 20 to 28 Myrs. Lithium dex fraction is presented at appropriate age. The last column provides effective temperature to outline composition impact on it.

	Z (mass fraction)	Y (mass fraction)	α	^7Li content (dex)	[O/Fe]	Tachocline	T_{eff} (K)
Solar models							
Reference	$1.959\ 10^{-2}$	0.2722	1.766	2.0	0	No	5776 K
Tachocline 1	$1.903\ 10^{-2}$	0.2695	1.748	0.35	0	Yes $\tau_{disk} = 0.5$	5777 K
Tachocline 2	$1.903\ 10^{-2}$	0.2695	1.748	1.1	0	Yes $\tau_{disk} = 10$	5777 K
Pleiades models							
A	$1.632\ 10^{-2}$	0.2624	1.766	2.6	0	No	5717 K
B	$1.632\ 10^{-2}$	0.2624	1.935, 1.850, 1.766	2.4	0	No	5715 K
C	$1.535\ 10^{-2}$	0.2679	1.766	2.75	0	No	5801 K
Hyades models							
A	$2.367\ 10^{-2}$	0.2633	1.766	0.9	0	No	5450 K
B	$2.367\ 10^{-2}$	0.2633	1.935, 1.850, 1.766	0.5	0	No	5466 K
C	$2.180\ 10^{-2}$	0.28	1.766	1.75	0	No	5646 K
D	$2.28\ 10^{-2}$	0.283	1.766	1.55	0	No	5632 K
E	$1.57\ 10^{-2}$	0.26	1.766	2.64	-0.2	No	5802 K
F	$1.94\ 10^{-2}$	0.26	1.766	1.98	-0.2	No	5638 K
G	$1.57\ 10^{-2}$	0.26	1.766	2.3	-0.2	Yes $\tau_{disk} = 10$	5805 K
H	$1.57\ 10^{-2}$	0.26	1.766	1.75	-0.2	Yes $\tau_{disk} = 0.5$	5804 K

temperature uncertainty of $\sim 250K$ and an abundance uncertainty of 0.11 dex. Figures 5 and 6 clearly show that such uncertainties are not large enough to recover agreement to computations. As we mainly analyze $1M\odot$ evolution, we concentrate on corresponding error-bars. It is generally found in litterature that these stars verify $0.6 < (B-V) < 0.75$. In fact, lithium abundances are such steep functions of effective temperature that if we use this criterium, we gather in the same sample stars with very different ^7Li fractions. Let us consider Hyades case. In Thorburn et al. (1993) data, the mean value of lithium content for stars exihibiting $0.6 < (B-V) < 0.75$ is $N(^7Li) = 2.0 \pm 0.6$ dex, but if we limit to $5400K < T_{eff} < 5500K$ which is what we get in computation, we get $N(^7Li) = 1.3 \pm 0.1$ in the same data set. The small sample presently discussed greatly reduces differences between observations and numerical predictions. Yet differences are not definitively cancelled out, and it is obvious from figure 5 and 6 that such possible misleading associations between stellar mass and (B-V) will not succeed in explaining the very large observation/theory gap concerning lower mass stars.

Table 2 shows that expected dispersions among metallicity or uncertainties on helium fraction can be responsible for dispersion of lithium abun-

dances. In Pleiades case, the metallicity variation from -0.034 dex (Z= 1.632 10^{-2}) to -0.058 dex (Z= 1.535 10^{-2}) minimal value corresponds to 6% in metal mass fraction and produces 0.35 dex variation in photospheric lithium, which is quite the order of observed dispersion for solar mass stars within this cluster. In Hyades case, helium uncertainties at a level of $\sim 7\,\%$ correspondingly produce 0.6 dex ^7Li dispersion between models types (A) and (D). Composition variations are therefore able to explain ^7Li dispersion through pre-MS initial depletion effect but mass accretion could contribute to it also (section 4). If such variations explain lithium dispersions in young Pleiades or Coma clusters they also have to deal with middle-aged cluster observations. In Hyades dispersion in the $T_{eff} - ^7Li$ relation has considerably decreased.

3.5. Opacity role on ^7Li burning

Because of strong dependence of lithium pre-MS depletion on metallicity opacities effects in stellar interiors have been studied (Turck-Chièze et al., 1993; Turck-Chièze 1998; Turcotte & Christensen-Dalsgaard 1998). Solar-like star metal opacities increase is responsible for the transition between radiative and convective energy transport. In the present Sun, the main contributors to the opacity at BCZ are oxygen and iron. They correspond respectively to 36 and 20 % of the total opacity (table 3). Situation is somewhat similar regarding pre-main sequence but the principal metal contributors to opacity are not the same because the medium is denser and hotter. The roles of oxygen and iron are of the same order of 20 %, then neon, silicium, and magnesium each represent approximately 10 % of total opacity.
Up to now we have deduced metallicity from [Fe/H], in keeping the solar distribution inside the metals. There have been hints that solar abundances may deviate from mean ISM abundances and that solar system would not be representative of general trends (Gies & Lambert 1991). Regarding open clusters, similar situation could appear even if direct determinations have to be considered cautiously due to chromospheric activity see Cayrel et al. (1985) for Hyades. Let us consider Hyades cluster. It is the closest and probably the best documented. Moreover it appears metal-rich. Hence Hyades stars experience amplified early pre-MS ^7Li depletion. As we have already

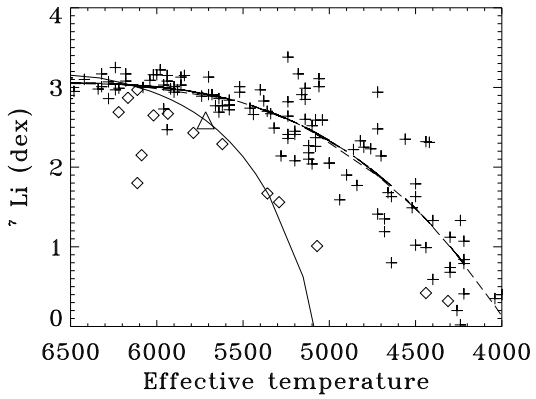

Fig. 5.— Crosses : ^7Li abundances for members of the Pleiades (Soderblom 93 data). Diamonds : Coma Berenices (Jeffries & James 99 data). Solid line is prediction of standard (corresponding to model Pleiades A) model of Pleiades composition. Small triangle on this line is $1M_\odot$ star of pleiades composition. Dashed-line is lithium fraction interpolation in Pleiades.

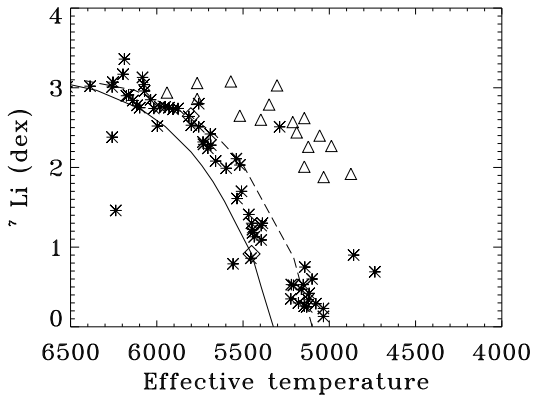

Fig. 6.— Crosses : ^7Li abundances for members of the Hyades (Thorburn 93 data). Triangles : Blanco I (Jeffries data). Lines show model computation for different masses at ~ 625 Myrs. Solid line is prediction of standard (corresponding to model Hyades A) model of Hyades composition. Dashed line is prediction of case E model (see section on opacities). Small diamonds on both lines represent $1M_\odot$ star.

said, predominant metals in opacity generation are iron, oxygen, neon, silicium, and magnesium. The full set of these metals represents more than 70% of total opacity whereas any other accounted for metal do not contribute over 5%. In table 3 we give opacity contributions of 19 metals at BCZ for a $1M_{\odot}$ star extracted from monochromatic calculations of Iglesias & Rogers (1996). Those results are obtained the following way : for every component we compute total opacity for the stellar plasma mixing excluding that component. Difference of opacity with the plasma including every components then allows to estimate to what level that element is responsible for opacity.

Table 3: Repartition of elements in opacity calculations at BCZ for solar composition in typical main sequence (T $\sim 2.10^6$K$\rho \sim 0.2$g.cm^{-3}) and pre-main sequence (T $\sim 4.10^6$K$\rho \sim 2$g.cm^{-3}) conditions.

Element	MS	pre-MS
H	20%	13%
He	11%	6%
C	8%	2%
N	5%	1%
O	36%	19%
Ne	9%	13%
Mg	3%	11%
Al	$< 1\%$	1%
Si	3%	12%
S	4%	5%
Ar	1.5%	$< 1\%$
Ca	2%	$< 1\%$
Fe	16%	22%
Ni	1%	2%
For every following metal Na,P,Cl,K, Ti,Cr and Mn	$< 1\%$	$< 1\%$

We now try to determine the detailed composition of the Hyades for relevant metals. Edvardsson et al.(1993) find a tight correlation between [O/Fe] and [Fe/H] in galactic disk stars,
$[O/Fe] = (-0.36 \pm 0.02) \times [Fe/H] - (0.044 \pm 0.010)$
This relation once again suggests our Sun could be overabundant in oxygen when compared to other stars. Moreover Garcia Lopez et al. (1993) claim oxygen to hydrogen metallicity is close to $[O/H] = -0.07 \pm 0.05$ dex in solar-like Hyades stars. This result is qualitatively consistent with the previous relation. If we apply this law, Hyades appear now metal-poor in oxygen compared to the Sun, this is in agreement with helium determinations from Perryman et al. (1998). Neon is not detectable in solar-like stars photosphere but its ratio to oxygen measured in HII regions is remarkably constant for different [O/H] (Meyer 1989). Indeed neon, silicium, and magnesium are expected to vary like oxygen because of their common origin in SNII. Consequently we decide to take the same variation for silicium and magnesium than for oxygen. Let us just signal one caveat regarding silicium : Cayrel, Cayrel de Strobel, &Campbell 1985 find $[Si/H] = 0.16 \pm 0.05$. Carbon cannot be ignored at least on MS but its origins are still a matter of debate (Gustafsson et al. 1999). We let it vary like oxygen.

We have generated opacity tables for this non-solar metal distributions using the devoted Lawrence Livermore National Laboratory website. By doing so we have chosen to model two cases. In the first one (case E), every metal varies like oxygen except iron-peak elements; in the second case, we let every metal vary like iron except the oxygen, to test the dependence of lithium depletion on oxygen (case F). In case E, which is the most realistic, lithium abundance is 2.6 dex (instead 0.9 dex) for a $1M_{\odot}$ star. The shift of oxygen abundance from 0.127 to -0.07 dex increases lithium fraction by a large amount of 1.1 dex. Then the shifting of every metal but iron-peak ones to the level of oxygen increases again lithium fraction by 0.6 dex. This dramatic increase in lithium fraction is shown on figures 6 and 7. Lithium in solar-like Hyades stars becomes quite compatible with observations. There are two reasons for this. First, the decrease in metal fraction reduces BCZ temperatures and secondly it increases effective temperature for any given mass. Solar mass stars are shifted from ~ 5450 to ~ 5800 Kelvins. The large effect of metal might at first seem worrying. However one as to keep in mind two points. Firstly metals determine roughly 80 % of opacities

at BCZ during pre-MS. Secondly lithium depletion is a very steep function of temperature (see figure 3). Furthermore we remark that such a large impact of metallicity on depletion is reported in other recent studies (Chaboyer, Demarque, & Pinsonneault 1995). Ventura et al. 1998 use OPAL opacity table although a slightly older version. They claim a decrease of 15% in the value of Z (around Z=0.02) makes the ^7Li abundance to vary by almost two orders of magnitude. The present effect of oxygen (0.2 dex represents $\sim 60\%$) which is half of metal fraction is quite compatible with this last result.

We note that even lower mass stars appear in good agreement with observations. Figure 7 outlines the importance of metals in lithium depletion. It also shows that oxygen plays a more determinant role than iron for pre-mainsequence evolution.

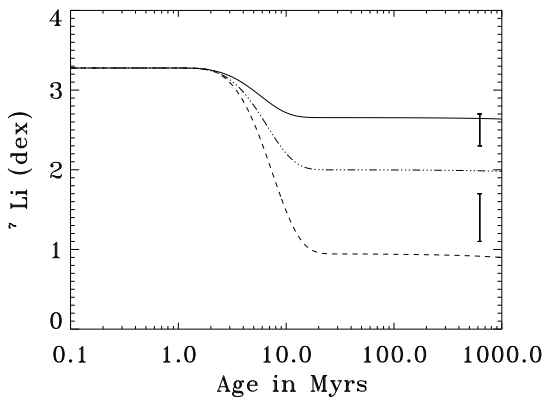

Fig. 7.— Predictions compared to observations for solar-like stars of Hyades composition. Solid line corresponds to Hyades' composition with every metal scaled on oxygen [O/H]=-0.07 dex except iron-peak elements (case E). Dashed line corresponds to model where all metal are scaled on iron [Fe/H]=0.127 dex (case A). For dashed dot line all metal are scaled on iron except oxygen (case F). Error-bars photospheric observed lithium are deduced from Thorburn et al. (1993) data for solar-type stars considering T_{eff} within 100 K around 5450 K (case A) and around 5800 K (case E).

If opacities are crucial at the base of convection zone they are also of first importance in the atmosphere, as they determine depth where material becomes convective and this affects significantly the convection zone extension. The deeper convection starts in atmosphere the more efficient it is and the deeper it goes in the envelope. For low effective temperatures encountered on the Hayashi track many contributors to opacity have to be considered. The lowest temperature we reach in computation is 3200 K and below 5000 K molecules are not negligible anymore. It is therefore likely that improvements of present models may be made when using new atmosphere models (Hauschildt, Allard, & Baron 1999). Here we have mainly use Alexander & Ferguson opacity tables (Alexander & Ferguson 94) and checked that there was no important discrepancy induced when using low-temperatures Kurucz opacity tables (Kurucz 1992). For case A composition star, final (and maximal) difference between otherwise similar models is less than 0.1 dex which is very small if we recall global depletion factor is more than 2 dex in this case.

In typical pre-MS conditions H^- remains the main opacity source. The metals provide a larger part of free electrons when temperature lowers. Alexander & Ferguson opacity table have been computed for solar composition and is not adapted for case E. We can evaluate average ionisation states of all components in atmospheric thermodynamic conditions. For the coldest ($\sim 3164K$) and most diffuse ($1.5\,10^{-10}$g.cm^{-3}) conditions, iron-peak elements and oxygen are respectively responsible for $\sim$ 10 and 0.25 % of electron density. When opacity evaluation changes from Alexander to OPAL table, temperature is logT=3.75 and density is typically a few 10^{-7} g.cm^{-3}. We estimate iron-peak elements to be responsible for ~ 30 % of electron density and contribution of oxygen being negligible.

In case E metal fraction is reasonably scaled by oxygen which is the main mass contributor for heavy elements. Case E is therefore slightly warmer than case A model and its BCZ is at a lower temperature. At $\sim$ 6 Myrs case A BCZ is located at $0.3M_\odot$ where $T = 3.99\,10^6K$ case E BCZ is located at $0.4M_\odot$ where $T = 3.72\,10^6K$. On the other hand by scaling every metal on oxygen we underestimate iron-peak element fraction (and effects) in the atmosphere where they could

provide up to 30 % of free electrons. If the right iron-peak element fraction was considered in the atmosphere, electron density would be enhanced. Convection would start closer to the surface and would therefore be less efficient. So we can expect that our values of BCZ temperature are in case E a bit too high. Figure 8 shows however that the changes among metal fractions are mainly felt at BCZ. Difference in temperatures as a function of mass never exceed 5% and changed opacities mainly affect BCZ but not the global structure.

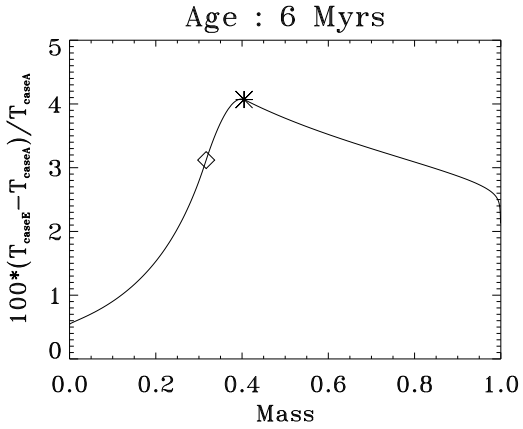

Fig. 8.— Relative temperature difference at a given depth between case E and case A models. Diamond and cross respectively locate BCZ of case A and E models.

4. MACROSCOPIC EFFECTS: CONVECTION AND ACCRETION

4.1. Efficiency of convection

The usual mixing-length theory parameter value relies on solar calibration. There is no reason to believe it is universal. Recent work based on hydrodynamical simulations (Ludwig et al. 1999) has investigated possible calibrations of mixing-length for solar-type stars. This work shows a dependence of α on effective temperature and surface gravity. For temperatures between 7100 and 4300 K and surface gravities 2.54 <log g< 4.74 α varies from 1.3 to more than 1.7. Using this work we find negligible evolution of α on the Hayashi track for a 1 $M_\odot$ object where surface gravity varies significantly but effective temperature remains almost constant. On the contrary once the radiative core becomes important and the star leaves the Hayashi track, the increase of the effective temperature could justify a change of the α value. For a solar composition model this occurs at about 12 Myrs ie slightly before the end of the ^7Li burning phase. In order to follow the effective temperature impact on α we have computed models of 1 $M_\odot$ stars for Pleiades, solar, and Hyades composition. Effective temperature being sensitive to composition age and α parameters vary with both of them. Temperature differences on the Hayashi track are approximately 70 K if one changes from solar to Hyades composition. In region of interest in temperature and gravity, differences in α are not significant over such a narrow temperature range and the same α can be used. After leaving the Hayashi track temperature differences increases up to 200 K but the star evolves towards solar main sequence conditions in a zone where there is a 'plateau' in α (Ludwig et al. 1999). Here again one can adopt a unique value so that for present study the change in α corresponds to temperature and not composition. On this point Ludwig et al.(1999) agrees with Fernandes et al. (1998) results who found that α is almost constant in the Sun and 4 low-mass stars systems having metallicities between solar and -0.31 dex, and helium content from 0.25 to 0.28. For these reasons we use the same values in the mixing length parameter whatever the composition. Pleiades and solar composition being close, we only made distinction between this group and Hyades. Between these two groups composition determines the time spent on the Hayashi track. We have considered three different α values: on the Hayashi track, when the radiative stratification begins to influence surface temperature and on the main sequence where the value results from usual solar calibration. Following Ludwig et al. advices we have adopted α values they proposed after reestimate by 0.1 and use their values as scaling factors. If the star has solar or Pleiades composition, α=1.935 before 15 Myrs ; α=1.85 between 15 and 22 Myrs and α=1.766 after 22 Myrs which is our solar-calibration main sequence value. If the star has Hyades composition, we use the same values but at different times and change the limits to 20 Myrs and 28 Myrs. Higher metallicity results in slower contraction and evolution. In Hyades case only the initial value of α

is important because after 20 Myrs ^7Li burning is over.

Results of the hydrodynamical calibration must be considered cautiously. Firstly, because low temperatures molecular opacities are not included in Ludwig et al. calculations and we are presently exploring low effective temperatures regions. Secondly a recent result about ι Pegasi binary systems calibration predicts opposite evolution of α with effective temperature (Morel et al 2000). Thirdly 2D calculations have to be confirmed by 3D hydrodynamical calculations.
In these calculations, ^7Li depletion is increased (table 2, case B) as convection zone extends deeper to higher temperatures with more efficient convection. We note nevertheless that such modification leads to less lithium destruction than using a full spectrum of turbulence as Ventura et al. (1998).

4.2. Mass accretion

Observations of T Tauri stars accretion luminosities lead to mass accretion rates spanning from a few 10^{-8} up to a few $10^{-6}\,M_\odot$/yr (Hartigan 1995, Gullbring et al. 1998). This wide range probably originate from real star to star differences altough such low accretion rates are very difficult to evaluate (Hartmann 1997) and suffer from large uncertainties. Accretion can affect ^7Li stellar photosphere abundances in mainly three different ways. First, it has a structural impact as it modifies the stellar mass, consequently the gravitational potential then stratification change. Secondly, providing ISM abundance material to the surface of the star, has a direct chemical impact. Thirdly, accretion should also change stellar boundary conditions which is probably the most difficult part of the accretion phenomenon to modelize.

Our hydrostatic calculation takes accretion into account in a crude fashion. The accreted mass modifies only the external layers of the star and does not directly affect global surface boundary conditions (pressure, temperature, luminosity). Mass is simply added on the outermost layer of the star. We limit our study to accretion rates below $10^{-7}\,M_\odot$/yr and following Hartmann (1997), we consider global accreted mass of a few $10^{-2}\,M_\odot$. As recent hints suggest that accretion could last longer than usually believed and perhaps deal with larger accreted masses (Muzerolle et al. 2000), so we will then also investigate the effects of $0.1M_\odot$ mass accreted.

4.3. A low global accretion mass

We first evaluate ^7Li photosphere variations through accretion by simply considering different nonaccreting stellar masses. For a 2% accretion mass, if the structural effect is dominant, final minimal ^7Li photosphere fraction is the one of 0.98 $M_\odot$ non-accreting star. This minimal fraction is 1.92, to compare with 2.13 for a 1 $M_\odot$ for a solar composition. Then the maximal fraction can also be evaluated, if we consider that the chemical mixing is dominant. This value is obtained in considering a $1M_\odot$ star but artificially increase ^7Li photosphere fraction by diluting in external CZ the ^7Li mass contained in $0.02M_\odot$ of ISM material. The ^7Li maximal fraction is 2.61 for a 1 $M_\odot$.

A real accreting star has a lower mass all the way through accretion phases and depletes both its initial lithium and lithium it receives from accretion. So, in the following we consider accretion impact on ^7Li burning for solar composition star and 2% $M_\odot$ total accreted mass at varying temporal rates. Starting with a 0.98 $M_\odot$ stellar object we consider a 'fast accretion' rate model of $10^{-8}M_\odot$/yr during 2 Myrs, we get a lithium content of 2.12 dex and then a 'slow accretion' rate model $10^{-8}M_\odot$/yr and $10^{-9}M_\odot$/yr during 1 and 10 Myrs respectively which gives a lithium content of 2.08 dex. This kind of simulation does not affect depletion by more than 0.05 dex. The general trend of accretion is to lower ^7Li fraction so we can conclude that structural effects are predominant over chemical effects. The effect is neither sufficient to recover the agreement with observational ^7Li fraction nor to explain the spread in young clusters.

Accretion will have different consequences on lithium burning if it could last long enough ie after major ^7Li pre-MS depletion phase. Near IR excess of very low accretion rates of $10^{-9}M_\odot$/yr are currently not dectected (Hartigan, Edwards, & Ghandour 1995). The simple evaluation we make just above illustrates that a variation of only very few percent of stellar mass could have a nonnegligible chemical impact because after 10 Myrs external convection zone is 10 % or lower of the stellar mass. Then, an accretion rate as low

as $10^{-9} M_{\odot}$/yr could significantly change ZAMS lithium surface fraction.

4.4. Larger accretion rates applied to the Pleiades composition

90% or more of stellar final mass is accreted during short (less than one myr) class 0 and class I stages who extend up to a few 10^5 years before classical T Tauri phase (Andre, Ward-Thomson, & Barsony 1999 and references therein). We consider here both different final masses from 0.9 to 1.1 $M_{\odot}$ and different globally accreted masses ie $2\,10^{-2}$ or $10^{-1} M_{\odot}$. The stars now have Pleiades composition. As we have seen in the solar case, structural effect of accretion is maximum when accretion is fast, we therefore restrict our computation to 'fast' accretion process: 10^{-8} or $5\,10^{-8} M_{\odot}.\mathrm{yrs}^{-1}$ during the first Myr and then 10^{-9} or $5\,10^{-9} M_{\odot}.\mathrm{yrs}^{-1}$ from 1 to 11 Myrs. In these conditions, accretion still increases ^7Li depletion and confirms solar trend. In table 4 we give lithium abundance relative to hydrogen as function of mass and with or without accretion in case of Pleiades. The lower the mass the higher the accretion impact. Accretion could therefore explain initial lithium dispersion that also seem to increase towards low effective temperatures.

Table 4: Lithium surface abundances at 70 Myrs for accreting and non-accreting Pleiades composition models.

Mass	$1.1 M_{\odot}$	$1 M_{\odot}$	$0.9 M_{\odot}$
Effective temperature	6050	5720	5350
Observed mean lithium abundance	2.92	2.70	2.57
No accretion models	2.95	2.58	1.66
Global accreted mass = $0.02 M_{\odot}$	2.94	2.56	1.59
Global accreted mass = $0.1 M_{\odot}$	2.86	2.39	1.24

For a comparison, we estimate observational lithium abundance dispersion in the data set of Soderblom et al. (1993) we divide into 200 K bins. For each bin we then compute mean abundance value and dispersion. Between 4200 and 6000 K, we find that dispersion varies from 0.65 to ~ 0.1 dex exhibiting the well-known general trend to decrease when tempature increases. Around T_{eff}= 5720 K (1 $M_{\odot}$) it is ~ 0.12 while around T_{eff}= 5350 K (0.9 $M_{\odot}$) it is ~ 0.32. As can be seen in table 4 these results are qualitatively and quantitatively comparable to predicted dispersion resulting from accretion of 10 % of $M_{\odot}$. We conclude that accretion could explain early main sequence dispersion. Results suggest also that the more a star accretes the more it depletes ^7Li because once again in these cases structural effects dominate chemical effects. ^7Li is not refreshed at a sufficient level to compensate for the additive burning due to the lower mass.

Table 5: Evolution in $M_{\odot}/yr$ of required accretion rates to reach lithium surface abundances at Pleiades age.

Age (myrs)	Accretion $1 M_{\odot}$	Accretion $0.9 M_{\odot}$
2	$6.3\,10^{-8}$	$7.9\,10^{-8}$
3	$6.3\,10^{-8}$	$7.9\,10^{-8}$
4	$4.0\,10^{-8}$	$6.3\,10^{-8}$
5	$3.1\,10^{-8}$	$4.0\,10^{-8}$
6	$1.6\,10^{-8}$	$2.0\,10^{-8}$
7	10^{-8}	$1.2\,10^{-8}$
8	$6.3\,10^{-9}$	$7.9\,10^{-9}$
9	$4.0\,10^{-9}$	$4.0\,10^{-9}$
10	$2.5\,10^{-9}$	$2.5\,10^{-9}$
15	$1.6\,10^{-10}$	$2.5\,10^{-10}$
20	$5\,10^{-12}$	$2.5\,10^{-11}$

We now evaluate the minimal accretion rate necessary to counteract mass effect for stellar masses of 0.9 and 1 $M_{\odot}$ (table 5). Every million years photosphere ^7Li fraction disminishes by a given amount and knowing convection zone mass and ISM ^7Li fraction we compute a 'nominal' mass accretion rate necessary to exactly compensate losses. One could however argue that 1 $M_{\odot}$ Pleiades have not kept initial ^7Li fractions. They indeed depleted from ISM value ~ 3.2 down to ~ 2.8. Taking this into account we compute a new accretion rate in the following way : if a fraction α of 'nominal' accretion is provided every Myr only $1-\alpha$ of the quantity of depleted ^7Li with no accretion will finally be depleted. We find

that new accretion rates should be lowered from 'nominal' ones by 0.32 dex and we provide results in table 5. Results do not really change within considered mass range. When compared to observations of present star forming regions (Calvet & Gullbring 1998; Muzerolle et al. 2000) these accretion rates seem slightly too high. The required accretion rates exceed strongest reported accretions observations by approximately 0.5 dex which brings us close to the observational upper limits.

It is clear that conclusion on the accretion rates requires improved detection of mass accretion estimates to rates as low as $10^{-9} M_{\odot}$/yr for a large number of very young clusters, especially for low mass stars and corresponding photospheric lithium content. Therefore preceding results are mainly illustrative rather than conclusive. Moreover, the accretion process has to be approached hydrodynamically and maybe in considering periodic phenomena, to take into account the modified boundary conditions.

5. MACROSCOPIC EFFECTS: THE INFLUENCE OF THE ROTATION

Regarding solar-like stars, open clusters ^7Li abundances suggest a general depletion over main sequence which is in contradiction with standard evolution codes results. We will examine in this section the role of the internal rotation firstly on the pre-mainsequence structure and secondly on the possible tachocline mixing process inside radiation zone.

5.1. Rotation structural effects

Within the last decade many theoretical works have been led in the field of angular momentum transport in stellar interiors. Such works encounter difficulties to explain rotation velocity evolution. For instance models invoking hydrodynamic angular momentum transport (Pinsonneault et al. 1989) predict strong differential rotation in solar interior which is contradictory with helioseismology results. Models with angular momentum transport induced by internal magnetic fields (Keppens, Mac Gregor, & Charbonneau 1995) can fit observations with a core-enveloppe coupling time of the order of 10 Myrs. They however encounter problems in reproducing the slowest rotators in open clusters and early MS rotational evolution.

Core rotation could still significantly differ from surface rotation. Rotation rate is presently observed to be constant in most of the solar radiation zone and varies with latitude in solar convection zone. However it could have been a varying quantity in the initial stellar radiative and/or convective interior. We investigate here purely structural effects of varying internal rotation and examine the consequences on effective temperature, luminosity, and lithium content. The models we consider have Hyades composition where the stars below $1 M_{\odot}$ all have experienced an initial rotational history increase until ZAMS followed by a strong decrease (see section 5.2). On the other hand they are still at the beginning of ZAMS so there is probably no long term MS effects on lithium. This cluster therefore seems to us quite appropriate to study early rotational effects. We compute three models in the case of very short-lived circumstellar disk of 0.5 Myrs. The first model (SBR), assumes solid body rotation throughout the star. The second (DR), assumes complete decoupling between radiative and convective zones and the last model (FR) assumes solid body rotation in convection zone and every stellar mass shell keeps its initial angular momentum in radiative stratification part. If the first model corresponds to zero coupling time between convection and radiation zones, this coupling time is infinite in the latter ones.

A well known structural effect of rotation is the decrease of the effective temperature and to a less extent of stellar luminosity (Sills, Pinsonneault, & Terndrup 2000). For the SBR stellar model we compute equatorial velocity of 74 km/s on ZAMS ($\sim 57 Myrs$). This gives rise to a temperature decrease of only 23 K in comparison with the nonrotating model. Under analog conditions, the polynomial formula of Sills et al. gives a discrepancy of 15 K. The same formula at maximal speed age (110 km/s for $\sim 30 Myrs$) leads to 50 K where we find 65 K in difference. Differences never exceed 0.03 dex in luminosity and 2 % in radius at given time. The expected consequence of such a behavior over convection is a larger extension and higher BCZ temperature and density responsible of the higher depletion rate in ^7Li. Temperature at the BCZ increases strongly when the effective temperature lowers. This mass-lowering is effec-

tive when the star reaches its maximal rotation rate around 30 Myrs. Yet before $\sim 7 Myrs$ the situation is reversed and rotation models surprisingly exhibit lower BCZ temperature and density. A maximum difference in temperature of $2\,10^4$K appears at 3 Myrs. It seems indeed that early rotational effects over BCZ are opposite to what they become afterwards. This trend changes the temperature sensitivity on ^7Li depletion rate.

Quantitative variation of lithium fraction between slowly (τ_{disk}=3 Myrs) and rapidly (τ_{disk} =0.5 Myrs) rotating models is very small : 0.1 dex (Table 6). No difference exists between SBR and DR models because the rotation is the same before 20 Myrs. In fact, the rotation rate, anywhere in the star, is independent of any coupling time at least until 20 Myrs and at this age ^7Li pre-MS depletion is over. There are two reasons for that. Firstly radiation zone stratification is still hardly under-adiabatic until 30 Myrs as we already explained in section 2.1. Secondly stellar wind loss represents only 12% of initial momentum at 20 Myrs (vs $\sim$ 99% at solar age). Contraction of the whole star therefore stays homologuous and coupling-time between zones has no impact. Unless initial conditions are different from solid rotation for the initial fully convective body there are no requirements to bother about angular momentum loss or exchanges during early pre-MS ^7Li burning phases.

In the preceding lines we have been concerned by structural effects as far as they result from a correction to local gravity. We do not note any significant impact of these effects on the present problem. Now there are others means by which rotation might affect stellar structure. Convective movements are sensitive to rotation through coriolis force. This effect is known for long in earthly atmospheric global circulation notably in the intertropical region. Siess & Livio 1997 suggest that convective cells could be twisted by rotation allowing therefore a smaller α_{mlt} to the convective zone. As long as precise hydrodynamical computation are led on that phenomenon it is however difficult to say much more about this solution.

5.2. The turbulence at the base of the convection zone

We consider now that the rotation induces an hydrodynamical instability in the tachocline layer at the top of the radiation zone (Spiegel & Zahn 1992). Such an instability has been studied by BTCZ99 to interpret the helioseismic results (Kosovichev et al. 1997) and could partly be at the origin of lithium destruction during the main-sequence. The introduction of a time dependent turbulent term in the diffusive equation permits a better agreement on solar photospheric light elements between observations and models. BTCZ99 remark that in the present Sun, tachocline mixing is thin enough not to deplete ^9Be. However tachocline mixing depends on rotation and differential rotation which is poorly known in pre-MS stars.
We reexamine this process introducing a more realistic rotation history in pre-MS. A $1M_\odot$ model of Hyades composition and including tachocline mixing will not deplete more than 0.03 dex in ^9Be from formation until ZAMS and none afterwards. Beryllium depletion does not occur although rapid rotation and high BCZ temperatures. It is the reason why we do not discuss ^9Be in this study.

Skumanich law (Skumanich 1972) has been used to infer rotational time evolution in main-sequence (as in BTCZ99). But such a law cannot be extend to young pre-MS stars which initially rotate slowly and then experience strong acceleration toward ZAMS. We reevaluate here tachocline mixing in using a more realistic rotation law that should apply over both pre-MS and MS. So we adopt the approach of Bouvier, Forestini, & Allain (1997, hereafter BFA97) to calculate different sets of rotation evolution for 1 $M_\odot$ stars under the three following assumptions : (i) stars rotate as solid bodies, (ii) stars are locked to a defined angular velocity as long as they interact with initial surrounding disk, (iii) magnetic wind braking acts all along pre-MS and MS and depending on rotation speed produces varying angular momentum loss rate:

$$(\frac{dJ}{dt})_w = -K\Omega^3(\frac{R}{R_o})^{1/2}(\frac{M}{M_o})^{-1/2} \text{ if } \Omega < \omega_{\rm sat} \quad (1)$$

$$(\frac{dJ}{dt})_w = -K\Omega{\omega_{sat}}^2(\frac{R}{R_o})^{1/2}(\frac{M}{M_o})^{-1/2} \text{ if } \Omega > \omega_{\rm sat} \quad (2)$$

Figure 9 presents corresponding equatorial ve-

Table 6: Impact of internal rotation model on lithium fraction in dex for solar mass and Hyades composition star

$\tau_{disk} in Myrs$	No rotation	SBR	DR	FR
Lithium at 7 Myrs	2.06	+0.11	+0.11	-0.01
Lithium at 20 Myrs	0.96	+0.07	+0.08	-0.07
Lithium at 0.7 Gyrs	0.91	+0.07	+0.07	-0.05

locity evolution for solar mass and composition. ω_{sat} and K are adjusted to fit observations of surface rotation rates. Surface magnetic field in solar type stars seems to increase with Ω up to $\sim 10\Omega_o$ and then saturates (Saar 1996). Saturation value determines a transition in the efficiency of the wind to brake the star which has consequences over early MS rotation rates. Following BFA97 we adjust ω_{sat}=14 Ω_o. K determines the rotation rate at solar age. Recent helioseismic measurements (Corbard et al. 1997) give internal solar rotation rates. A latitudinal dependence of rotation frequency is observed in convection zone, from 460 nHz at equator down to 370 nHz at 60 degrees latitude. Radiative zone then experiences rigid rotation at the 430 nHz level and at least as deep as 0.4 solar radius. In present solid rotation models, we adjust the rotational evolution laws so that the frequency is 430 nHz at solar age. To reach this rotation rate at actual solar age we adjust K to 3.25 $10^{47} g.cm^2.s$ in the expression of the braking law. This value is a little larger than the one used by BFA97 (2.7 $10^{47} g.cm^2.s$) as we tend towards a slower rotation velocity than surface equatorial : $2.7\,10^{-6} rd.s^{-1}$ instead of $2.9\,10^{-6} rd.s^{-1}$.

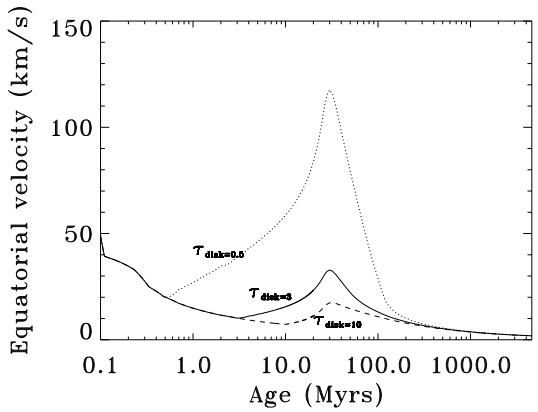

Fig. 9.— Equatorial velovity vs age for stars of solar mass and composition. From fastest to slowest rotators τ_{disk} is 0.5,3,10 Myrs.

We then consider three different τ_{disk} durations for star/disk coupling time : 0.5, 3, and 10 Myrs. 0.5 Myrs corresponds to a star that ceases disk locking evolution on its birthline or a few 0.1 Myrs after depending on mass and composition. Three Myrs is the median disk lifetime as estimated by BFA97. Finally 10 Myrs corresponds to a persistent disk. At this age only 10 to 30 % of young stars still show the IR and mm radio emission expected if an optically thick disk is present (Strom 1995). The star is kept on a velocity of $9.1\,10^{-6} rd.s^{-1}$ until it uncouples from disk. Then owing to gravitational contraction it accelerates up to $2.70\,10^{-5} rd.s^{-1}$ and $1.75\,10^{-4} rd.s^{-1}$ after ~ 30 Myrs for τ_{disk} equal 10 and 0.5 Myrs respectively. Such rotation rates correspond to equatorial velocities that span from 20 km/s to 120 km/s. Afterwards the stars decelerate rapidly towards the same low velocity whatever disk lifetime. At the Hyades age the stellar equatorial velocity is in the narrow range from 4 to 6 km/s.

Metallicity has direct impact on rotation evolution. We evaluate rotation history for three sets of metallicities : Pleiades, Sun, and Hyades. From the former to the later composition contraction time towards ZAMS increases. Peak velocities are reached later and are slightly lowered mainly due to higher moment of inertia and radius. A $1 M_\odot$ pleiad reaches maximal velocity at 29 Myrs whereas its Hyades conterpart reaches it at 33 Myrs. Moreover radius being a bit larger the wind braking affects more surface rotation. For a typical disk lifetime of 3 Myrs we estimate peak velocity to be 120 km/s and 113 km/s for Pleiades and Hyades compositions. These values are reached

around 29 and 33 Myrs respectively.

Purely structural effects of rotation have been included the same way as in the preceeding section. Rotational centrifugal acceleration effects are added to gravity. This modifies the equation of hydrostatic equilibrium and radiative gradient. At radius r and angular velocity ω, the present stellar code integrates the 'mean' effect of rotation by substracting $2r\omega^2/3$ to gravitation. Then rotation velocities are also taken into account in a macroscopic rotationally induced diffusion coefficient D_T (equation 14 in BTCZ99) and tachocline thickness d (equation 11 in BTCZ99) that determines tachocline mixing efficiency. These coefficients are assumed to follow the scaling laws (suggested by BTCZ99):

$$D_T \, \alpha \, \Omega^{0.75 \pm 0.25} \tag{3}$$

$$d \, \alpha \, \Omega^{(1.3 \pm 0.1)/4} \tag{4}$$

5.2.1. The solar case

Rotation induces a strongly increased depletion of photospheric ^7Li. Structural modifications do not play any significative role on pre-main sequence as well as on main sequence unless the stellar disk lifetime is very short. For a 3 Myrs disk lifetime we note no differences exceeding 0.1 dex in ^7Li between a model that includes rotation structural changes and a model that does not. Stellar structures and evolutions are similar. On the contrary rotationally induced mixing dramatically changes ^7Li history. The 3 Myrs disk lifetime star experiences an enhanced destruction of ^7Li during radiative core developpement phase when compared to non rotation model. ^7Li abundance is lowered from $\sim$ 2.1 dex without rotation down to $\sim$ 1.8 dex. This increases ^7Li depletion during pre-main sequence in comparison with previous calculations using only the Skumanich law (BTCZ99). But the final result is not much altered. ^7Li depletion depends on disk lifetime τ_{disk}. Variation is important between τ_{disk}=0.5 and 3 Myrs but more moderate for longer disk lifetimes (table 7, figure 10, and 11).

Typical scatter between long and short lived disk is 0.5 dex and tends to grow slightly on main sequence. This does not agree with open-cluster observations that shows no dispersion in ^7Li abundances from Pleiades to Hyades as can be seen on previous plots. On the other hand spread reappears in much older clusters as M67 (Jones, Fischer, & Soderblom 1999). With a photospheric lithium of 1.1 dex, the Sun is expected to have experienced a long-lived disk stars (figure 10), if this approach is correct. However one has to be very extremely cautious when drawing such conclusion. Pre-MS depletion phase is overestimated as young open-clusters observations suggest.

5.2.2. The Hyades case

Tachocline thickness and macroscopic diffusion coefficient depends on the rotation history and the metallicity. However if scaling laws of equations 3 and 4 are correct, we compute that differences in metallicity of 0.1 dex do not induce large enough modifications in rotation speed to significantly change tachocline diffusion coefficient or thickness in pre-MS. The general behaviour noticed for the Sun is also observed for this cluster. But the computation shows that higher velocity rotating stars do exhibit larger ^7Li depletion, this does not agree with present observations, indicating that rapid rotators have higher ^7Li rates as their slower counterparts (Soderblom et al. 1993 ; Garcia Lopez, Rebolo, & Martin 1994). This point suggests that tachocline mixing, as it is now introduced in calculations, and probably any mechanism that would mix radiatively stabilized layers on pre-MS, could be partly inhibited. It is noteworthy that low mass star rotation are presumably evolving slower. A 0.8 $M_\odot$ star should reach peak velocity at 50 Myrs. Moreover such a star will retain its angular momentum longer so that tachocline mixing retains longer efficiency. This brings the star the wrong way for it is the lighter stars that present the largest discrepancy in ^7Li content between current models and observations.

6. SUMMARY AND PERSPECTIVES

This study confirms that lithium offers an extremely interesting insight over solar-like stellar structure and evolution due to its low depletion temperature. There is presently a discrepancy between computations of classical stellar models and observations. Classical models predict no lithium depletion on main sequence whereas it seems to be observed in open-cluster lifetimes. It is reasonable to think that lithium evolution on main

Table 7: Lithium fraction in dex for solar mass and composition star as a function of circumstellar disk lifetime.

$\tau_{disk} in Myrs$	0.5	3	10	20
Lithium at ZAMS	1.34	1.80	1.90	1.92
Lithium at 0.7 Gyrs	0.84	1.43	1.56	1.61
Lithium at 4.6 Gyrs	0.35	0.95	1.10	1.16

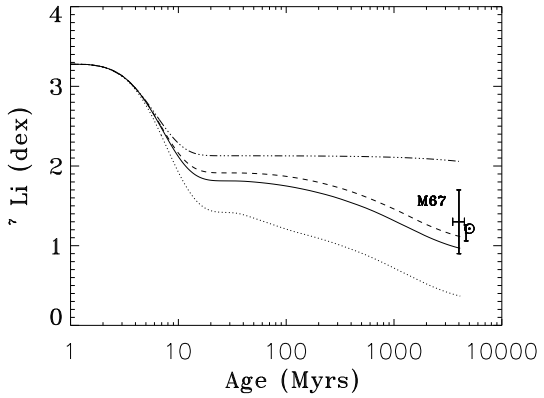

Fig. 10.— ^7Li surface abundances in solar mass and composition stars. From the lowest to the highest depletion rate : first model only includes microscopic diffusion and three following models add tachocline mixing with disk coupling time 10, 3, and 0.5 Myrs respectively. Also plotted M67 and solar surface lithium abundances. Every model exhibits the same effective temperature of 5777 K at 4.6 Gyrs (table 2 : solar models).

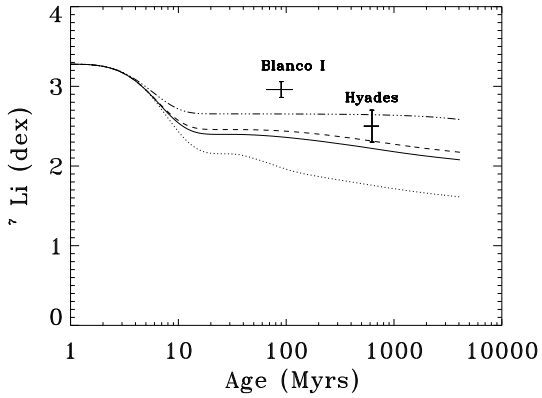

Fig. 11.— ^7Li surface abundances in solar mass and Hyades case E composition stars. Same presentation than above. Also plotted Blanco I and Hyades surface lithium abundances. Microscopic diffusion model has an effective temperature of 5802 K at 625 myrs. At this age all other models exhibit very similar effective temperatures (from 5800 to 5802 K)

sequence is connected to some slow mixing rotationally induced process(es) that occurs at the top of the radiative zone. In the specific case of our Sun such a process is supported by differences between theoretical and measured sound speed in this part of the star (BTCZ 1999) and by the agreement between photospheric observations and predictions for helium, metals, and lithium. During pre-mainsequence, the lithium problem is reversed and classical uptodate theoretical models generally predict too strong depletion. We confirm that this depletion strongly depends on metallicity, in the calculation. It is not evident that it is currently observed in young open-clusters. In this regard Coma Ber and Blanco I rather suggest an age dependence. Moreover, early dispersion in lithium abundances has to be explained.

In this paper, we have studied the impact of different microscopic or macroscopic processes on pre-MS lithium depletion. First we note the important role of the choice of meshes and time steps in the very early phase (before 10 Myrs). Secondly, we remark that the interpretation of data is presently difficult as ^7Li depletion in open-clusters is a strong function of effective temperature and it is therefore very difficult to reliably relate an observed lithium fraction to a given stellar mass just because this effective temperature depends on detailed metal fractions that still have to be accurately determined (see figure 6 compared to figures 7 and 11).

Microscopic processes are mainly dominated by opacity coefficients and therefore through metal and helium fractions. We experience in models that the level of sensitivity to composition (especially on oxygen and iron but not only) proves how difficult the present situation is. This suggests that the dispersion in lithium abundances could be related to small dispersion in metal fractions or among metal fractions. This is all the more true as part of the observed scatter is surely related to observational questions. Rotation history might induce such difference but on the other hand King, Krishnamuthi , & Pinsonneault 2000 note the ^7Li abundance determination to be correlated to (and probably biased by) chromospheric activity. Genuine dispersion could also be related to larger helium fraction variations which can not be ruled out even over small scales in the ISM (Wilson & Rood 94 and references therein). In the solar case, where all the abundances are known within 10%, we get the good order of magnitude of lithium depletion in adding a macroscopic effect to the implicit microscopic effect in pre-mainsequence. We do not observe also a large problem in Hyades when using observed oxygen and iron are measured. Nevertheless there is a contradiction between the large dependence of lithium depletion in theoretical models in comparison to the apparent quasi metallicity independence of the abundances in young open-clusters. To solve this problem we encourage measurements of photospheric abundances as carbon, oxygen, silicium, and iron on young T-Tauri stars. Similarly helium fraction needs to be carefully checked within clusters and if possible from star to star. Such additional data can be deduced from binary systems, high mass stars, and importantly in solar-like stars thanks to the future asteroseismology developments.

Macroscopic processes are at play through accretion, rotation, and convection modelling. Such processes are now crucial to understand accurately stellar evolution (Pinsonneault 1997). Accretion is likely to explain dispersion in ^7Li fraction measurements, but it fails to bring mean abundances to an acceptable level. In Pleiades case, required accretion rates at a given time are at the upper limit of observations for young T Tauri. To improve significantly the situation they should last so long that total accreted mass would indeed be $\sim 20-30\%$ of solar mass during the first Myrs following star formation. On the other hand it is also possible for young stars not to accrete from classical gas & dust disks but from planetesimals of protoplanetary systems which are not detectable today. Such material infall could supply lithium and others metals in low mass convective enveloppes of post-TTauri stars.

Rotationally induced mixing gives satisfactory results regarding photospheric solar lithium abundance. These results are moreover consistent with Hyades open-cluster observation when oxygen and iron fractions are correctly ie separatedly considered. Rotation mixing process we consider is however unable to explain initial spread in ^7Li surface abundances. Treating more properly the fruitful MS tachocline mixing (BTCZ 1999) in pre-MS leads to results not supported by observations (King, Krishnamurthi, & Pinsonneault 2000 and references therein) : we find a rotation-^7Li depletion correlation on ZAMS. However it is important to keep in mind two points. Firstly we recall that the present rotationally induced mixing is not related to angular momentum transport in the stars. It therefore offers a possible but certainly partial vision of lithium MS evolution. ZAMS rotational velocity should affect ^7Li depletion because of subsequent angular momentum redistribution (Pinsonneault et al. 1999 and references therein). Secondly the rotationally induced mixing process we invoke has necessary a transitory regime that we did not take into account. For these two reasons ^7Li depletion predictions of the tachocline mixing are more reliable between the Hyades and older clusters than absolute predictions from star formation. Hyades solar-like stars are already slow rotators and might have lost most of their angular momenta. From Hyades to older clusters, lithium should traduce long term (stationary) mixing effects, and indeed the tachocline mixing give rise to the observed characteristic time ($\sim 1Gyr$) for ^7Li depletion on MS.

Finally it is possible that the convection parameter α_{mlt} is sensitive to rotation and hydrodynamical simulations suggest it should be changed along Hayashi track. The effect we mention is not very large, contrary to some previous studies but more work is needed to be sure. We have emphasized the absence of a well established radiative stratification in central parts during phases preceeding 20 Myrs which is a tricky point. The

first phase of lithium burning occurs at the frontier between cooler convective medium and hotter radiative (but almost convective) medium that lies beneath. This means that very slight additional perturbation (through overshooting or instability for instance) could give rise to a much stronger lithium depletion. This also means that very slight stabilisation phenomenon, related to magnetic field as it is suggested by Ventura et al. (1998) could save a large fraction of lithium.

All these remarks on macroscopic phenomena encourage complementary studies implying hydrodynamics approach. This is also true to check if the star is initially fully convective and rotates as a solid body. The answers to those questions can only be extracted from earlier phases that include protostellar collapse and take into account hydrodynamical processes such as accretion in a consistent and more rigourous manner.

Acknowledments

Authors are grateful to Forrest Rogers and Carlos Iglesias from LLNL who made possible computation of opacity tables corresponding to non-solar repartition. They are also grateful to Jean-Paul Zahn for enlightening discussion on stellar structure and hydrodynamic instabilities and to Sacha Brun for strong interaction. We thank Sylvain Turcotte for his help on opacity and ionisation states calculations and we also thank Jean-Pierre Chièze Philippe André and Jean-Paul Meyer for giving some helpful advises on the fields of young stars physics and cosmic chemical abundances. Finally we are grateful to the referee for very interesting and helpful advices on the manuscript.

REFERENCES

Adelberger, E., et al., 1998, Rev. Mod. Phys., 70 (4), 1265

Alexander, D. R., Ferguson, J. W. 1994, ApJ, 437, 879

Andre, P., Ward-Thomson, D., Barsony, M. 1999, Protostars and Planets IV.

Basu, S., Antia, H. M. 1995, MNRAS, 276, 1402

Baglin, A., Morel, P., Schatzmann, E., 1985, A&A, 149, 309

Bodenheimer, P. H., 1965, ApJ, 142, 451

Boesgaard, A. M. 1987, ApJ, 321, 967

Boesgaard, A. M., &Friel, E. D. 1990, ApJ, 351, 467

Bouvier, J., Forestini, M., Allain, S. 1997, A&A, 326, 1023

Brun, A. S., Turck-Chièze, & Morel, P., 1998, ApJ, 506, 913

Brun, A. S., Turck-Chièze, S., Zahn, J. P. 1999, ApJ, 525, 1032

Calvet, N., &Gullbring, E. 1998, ApJ, 509, 802

Canuto, V. M., Goldman, I., Mazzitelli, I. 1996, ApJ, 473, 550

Cayrel, R., Cayrel de Strobel, G., &Campbell, B. 1985, A&A, 146, 249

Chaboyer, B., Demarque, P., Pinsonneault, M. H., 1995, ApJ, 441, 876

Corbard, T., Berthomieu, G., Morel, P., Provost, J., Schou, J., &Tomczyk, S. 1997, A&A, 324, 298

D'Antona, F., & Mazzitelli, I. 1984, A&A, 138, 431

D'Antona, F., & Mazzitelli, I. 1994, ApJS, 90, 467

D'Antona, F., & Mazzitelli, I. 1997, Mem. Soc. Astron. Italiana, 68, 807

D'Antona, F., Ventura, P. & Mazzitelli, I., 2000, ApJ lett., 543, L77

Deharveng, L., Pena, M., Caplan, J., &Costero, R. 2000, MNRAS, 311, 329

Deliyannis, C. P., Demarque, P., Kawaler, S. D., 1990, ApJS, 73, 21

Dziembowski, W.A., 1998, Space Sc. Rev., 85, 37

Engstler et al., Phys. Rev. Lett. B, 279, 20

Fernandes, J., Lebreton, Y., Baglin, A., Morel, P. ,1998, A&A, 338, 455

Friel, E. D., &Boesgaard, A. M. 1992, ApJ, 387, 170

Frohlich, C., et al. 1997, Sol. Phys., 170, 1

Gabriel, A. H., et al. 1997, Sol. Phys., 175, 207

Garcia Lopez, R. J., Rebolo, R., Herrero, A., &Beckman, J. E. 1993, ApJ, 412, 173

Garcia Lopez, R. J., Rebolo, R., &Martin, E. L. 1994, A&A, 282, 518

Gautier, D., &Morel, P. 1997, A&A, 323, L9

Gies, D. R., Lambert, D. L., 1992, ApJ, 387, 673

Gullbring, E., Hartmann, L., Briceno, C., Calvet, N. 1998, ApJ, 492, 323

Gustafsson, B., Karlsson, T., Olsson, E., Edvardsson, B., &Ryde, N. 1999, A&A, 342, 426

Hartigan, P., Edwards, S., Ghandour, L. 1995, ApJ, 452, 736

Hartmann, L., IAU Symposium No. 182, ed. Bo Reipurth and Claude Bertout. Kluwer Academic Publishers, 1997, p.391

Hauschildt, P. H., Allard, F., Baron, E. 1999, ApJ, 512, 377

Houdek, G., Rogl, J. 1996, Bull.Astr.Soc.India, 24, 317

Iglesias, C. A., Rogers, F. J. 1996, ApJ, 464, 943

Jeffries, R. D., 1999, MNRAS, 304, 821

Jeffries, R. D., &James, D. J. 1999, ApJ, 511, 218

Jones, B. F., Fischer, D., &Soderblom, D. R., 1999, AJ, 117, 330

Keppens, R., Mac&Gregor, K. B., &Charbonneau, P. 1995, A&A, 294, 469

King, J. R., Krishnamurthi, A., &Pinsonneault, M. H., 2000, AJ, 119, 859

Knauth, D. C., Federman, S. R., Lambert, D. L., Crane, P. 2000, Nature, 405, 6787, 626

Kosovichev et al., 1997, Sol. Phys., 170, 43

Kurucz, R. L., 1992, Rev. Mexicana Astron. Af., 23, 81

Lebreton, Y., 2000, ARA&A, 38, 35L

Linsky, J. L., Diplas, A., Wood, B. E., Brown, A., Ayres, T. R., &Savage, B. D. 1995, ApJ, 451, 335

Ludwig, H. G., Freytag, B., &Steffen, M. 1999, A&A, 346, 111

Magazzu, A., Rebolo, R., &Pavlenko, Y. V. 1992, ApJ, 392, 159

Meyer J.P., 1989, in: Cosmic Abundances of Matter, AIP Conference Proc. 183, C.J. Waddington ed., (Amer.Inst.Phys. ,NY), p. 245-303

Michaud, G., 1986, ApJ, 302, 650

Mihalas, D., Dappen, W., Hummer, D. G. 1988, ApJ, 331, 815

Minniti, D. 1995, A&A, 300, 109

Morel, P., van't Veer, C., Provost, J. Berthomieu, G., Castelli, F., Cayrel, R., Goupil, M. J., Lebreton, Y. 1994, A&A, 286, 91

Morel, P., A&AS, 1997, 124, 597

Morel, P., Morel, Ch., Provost, J., Berthomieu, G. 2000, A&A, 354, 636

Muzerolle, J., Calvet, N., Briceno, C., Hartmann, L., &Hillenbrand, L. 2000, ApJL, 535, L47 and Kylafis, Palla, F., 1999, in The origin of stars and planetary systems, ed. by Lada

Kluwer Academic, Publ., p 375.

Patenaude, M. 1978, A&A, 66, 225

Perryman, M. A. C., Brown, A. G. A., Lebreton, Y., Gomez, A., Turon, C., Cayrel&de&Strobel, G., Mermilliod, J. C., Robichon, N., Kovalevsky, J., &Crifo, F. 1998, A&A,331,81

Pinsonneault, M. H., Kawaler, S. D., Sofia, S., &Demarque, P. 1989, ApJ, 338, 424

Pinsonneault, M. H.,1997, ARA&A, 35, 557

Pinsonneault, M. H., Stauffer, J., Soderblom, D. R., King, J. R., Hanson, R. B. 1998, ApJ, 504, 170

Pinsonneault, M. H., Walker, T. P., Steigman, G., Narayanan, V. K., 1999, ApJ, 527, 180

Piskunov, N., Wood, B. E., Linsky, J. L., Dempsey, R. C., &Ayres, T. R. 1997, ApJ, 474, 315

Profitt, C. R., Michaud, G., 1989, ApJ, 346, 976

Rogers, F. J., Swenson, F. J., &Iglesias, C. A. 1996, ApJ, 456, 902

Saar,S. H., 1996, MHD phenomena in the Solar Atmosphere-Prototypes of Stellar Activity, IAU, Coll. 153, eds. Y. Uchida, T. Kosugi, p 237.

Schatzmann, E., 1993, A&A, 279, 431

Siess, L. & Livio, M., 1997, ApJ, 490, 785

Sills, A., Pinsonneault, M. H., &Terndrup, D. M. 2000, ApJ, 524, 335

Skumanich, A. 1972, ApJ, 171, 565

Soderblom, D. R., Jones, F. J., Balachandran, S. , Stauffer, J. R., Duncan, D. K., Fedele, S. B., &Hudon, J. D. 1993, AJ, 106, 1059

Stahler, S. W. 1988, ApJ, 332, 804

Thorburn, J. A., Hobbs, L. M., Deliyiannis, Constantine. P., &Pinsonneault, M. H. 1993, ApJ, 415, 150

Turck-Chièze, S., et al., 1997, Sol. Phys., 175, 247

Turcotte, S., Richer, J., Michaud, G., Iglesias, C. A., &Rogers, F. J. 1998, ApJ, 504, 539

Ventura, P. , Zeppieri, A. , Mazzitelli, I., D'Antonna, F. 1998, A&A, 331, 1011

Wilson, T. L., Rood, R. T. 1994, ARA&A, 32, 191

Zahn, J.P., 1974, in Stellar instabilities and Evolution, ed. P. Ledoux, A. W. Rogers; Reidel, p 185

Zahn, J.P., 1992, A&A, 265, 115

Zappala, R. R., 1972, ApJ, 172, 57

This 2-column preprint was prepared with the AAS LaTeX macros v5.0.